Original Article

Institution of MECHANICAL ENGINEERS

Journal of RISK AND RELIABILITY

Proc IMechE Part O:
J Risk and Reliability
1–14

DOI: 10.1177/1748006X19825593
journals.sagepub.com/home/pio

SAGE

Analyzing uncertainties in model response using the point estimate method: Applications from railway asset management

Thorsten Neumann[1], Beate Dutschk[2] and René Schenkendorf[3]

Abstract

Predicting current and future states of rail infrastructure based on existing data and measurements is essential for optimal maintenance and operation of railway systems. Mathematical models are helpful tools for detecting failures and extrapolating current states into the future. This, however, inherently gives rise to uncertainties in the model response that must be analyzed carefully to avoid misleading results and conclusions. Commonly, Monte Carlo simulations are used for such analyses which often require a large number of sample points to be evaluated for convergence. Moreover, even if quite close to the exact distributions, the Monte Carlo approach necessarily provides approximate results only. In contrast to that, the present contribution reviews an alternative way of computing important statistical quantities of the model response. The so-called point estimate method, which can be shown to be exact under certain constraints, usually (i.e. depending on the number of input variables) works with only a few specific sample points. Thus, the point estimate method helps to reduce the computational load for model evaluation considerably in the case of complex models or large-scale applications. To demonstrate the point estimate method, five academic but typical examples of railway asset management are analyzed in more detail: (a) track degradation, (b) reliability analysis of composite systems, (c) terminal reliability in rail networks, (d) failure detection/identification using decision trees, and (e) track condition modeling incorporating maintenance. Advantages as well as limitations of the point estimate method in comparison with common Monte Carlo simulations are discussed.

Keywords

Uncertainty propagation analysis, reliability, asset management, prognostics and health management, point estimate method

Date received: 15 February 2018; accepted: 14 December 2018

Introduction

Prognostics and health management (PHM) aims at increasing the reliability of technical systems and fostering their availability and safety with adequate and cost-efficient maintenance.[1] This, in particular, requires suitable models for diagnosing (i.e. fault detection, isolation, and failure mode identification[1,2]) and predicting degradation and potential failures of the system components based on available data and measurements which very often are uncertain. Due to the universality of the approach and not least because of its (financial) relevance for the industry, PHM has been applied in many technical disciplines thus far, including health management for batteries,[3] wind turbines,[4] nuclear power plants,[5] as well as bridges[6] or other infrastructures.

Regarding railway systems, preventive and condition-based maintenance of the tracks, as well as of the control and signaling equipment, is a crucial aspect in reducing interruptions and delays in train operations. Given its optimal implementation, it helps

[1]Institute of Transportation Systems, German Aerospace Center (DLR), Berlin, Germany
[2]Institute of Industrial Information Technology, Karlsruhe Institute of Technology (KIT), Karlsruhe, Germany
[3]Institute of Energy and Process Systems Engineering, Technical University of Braunschweig, Braunschweig, Germany

Corresponding author:
Thorsten Neumann, Institute of Transportation Systems, German Aerospace Center (DLR), Rutherfordstr. 2, 12489 Berlin, Germany.
Email: thorsten.neumann@dlr.de

to lower maintenance costs by avoiding expensive instant repairs when sudden failures, including possible incidental damages, occur. To be effective in this context, asset managers not only need to estimate the current health state of the rail infrastructure and its components, but they also need to predict future conditions based on available knowledge.

For instance, there is a significant interest in modeling track conditions and their temporal evolution[7–9] because track geometry directly influences comfort and safety in train operations potentially making immediate maintenance inevitable. Furthermore, predictions of the remaining useful life (RUL) of rail infrastructure components are very helpful or even necessary to derive optimal maintenance strategies.[10] In this context, system redundancies in terms of routes (or parallel tracks) in the overall network (macroscopic view) as well as with regard to the technical layout of a given infrastructure element (microscopic view) are an essential feature that allows keeping on operation also in case of individual failures. As a consequence, asset managers have to consider not only the reliability of single components but also composite systems.[11] Finally, automatic failure detection and identification helps to prioritize necessary repair activities and allocate related resources effectively. Besides some rule-based approaches,[12] decision trees,[13] as well as more advanced expert systems (e.g. based on big data and artificial intelligence),[14] have shown to be useful tools in this context.

Note that nearly all above-mentioned tasks usually require probabilistic elements in the models used because of the stochastic nature of failures, RUL, and asset degradation, for instance. This, of course, means that the resulting stochastics in the output of such models need to be taken into account as well. That is, quantifying the uncertainty in the model results essentially helps to make better decisions in maintenance planning.[1,8]

Commonly, Monte Carlo (MC) simulations are used to analyze the stochastic distribution of the model response whenever analytical solutions are not available or are difficult to obtain.[15] In contrast to that, an interesting alternative for numerically deriving important statistical quantities related to the model results (such as the mean or standard deviation) is given by the so-called point estimate method (PEM).[16,17] Given a model $f : \mathbb{R}^n \to \mathbb{R}^l$ with uncertain inputs and/or parameters X (where X is a random variable with values in $\mathbb{R}^n$), the basic idea of the PEM is to consider very specific realizations $x^{(1)}, \ldots, x^{(N)} \in \mathbb{R}^n$ of X instead of random samples (as in the standard MC approach) and then suitably weighting the model outputs $y^{(i)} = f(x^{(i)})$ or proper variants of it in order to obtain the requested assessment of the uncertainty in the model response $Y = f(X)$. By that, usually a substantial reduction of the number (i.e. N) of sample points to be evaluated is achieved which consequently means that—depending on the model under consideration—the PEM has the potential to considerably speed up the calculation of relevant basic statistics of the model response in case of large-scale applications, in particular. Moreover, note that the PEM results are easily reproducible (and sometimes even exact) because of deterministic sampling. In contrast to that, the convergence-based approach of MC simulations refers to (typically non-reproducible) finite random samples and thus necessarily yields more or less accurate, but approximate results on a random basis only. A detailed description of the proposed methodology follows in the next section before several numerical examples related to railway asset management are discussed.

Methodology

Let $f : \mathbb{R}^n \to \mathbb{R}^l$ be a mathematical function (or model) mapping an n-dimensional probabilistic input vector $X = (X_1, \ldots, X_n)^T$ with given distribution $\mathbb{P}^X$ on the l-dimensional model response $Y = f(X)$, where the X_i for $i = 1, \ldots, n$ are stochastically independent random variables. Thus, Y is a random variable, too, whose distribution $\mathbb{P}^Y$ usually is unknown. Without loss of generality, let $l = 1$ in the following as analyzing $f = (f_1, \ldots, f_l)^T$ at large is equivalent to analyzing its one-dimensional components $f_1, \ldots, f_l$ separately instead. Then, the PEM can be used for estimating the most important statistical quantities of $\mathbb{P}^Y$, such as mean or variance as a representation of the uncertainty in the model response, that is

$$\mathbb{E}(Y) = \mathbb{E}(f(X)) = \int_{\mathbb{R}^n} f(x) pdf_X(x) dx \tag{1}$$

and

$$\mathrm{Var}(Y) = \mathrm{Var}(f(X)) = \int_{\mathbb{R}^n} (f(x) - \mathbb{E}(f(X)))^2 pdf_X(x) dx \tag{2}$$

where $pdf_X : \mathbb{R}^n \to \mathbb{R}$ is the probability density function of X. Of course, other quantities that are described by similar integrals such as higher order (centralized) moments, for instance, can be considered as well.

Needless to say, depending on f and the distribution of X, it can be very difficult or even impossible to solve these integrals analytically. This, in particular, holds whenever f is given as a simulation or *black box* model only without any tractable analytical representation. For that reason, the PEM tries to find suitable approximations based on a small set of sample points that are defined by so-called generator functions $\mathrm{GF}[\cdot]$. For instance, when X is a three-dimensional standard Gaussian random variable with stochastically independent components (i.e. $X_i \sim \mathcal{N}(0,1)$ for $i = 1, 2, 3$), the first three generator functions are defined by

$$\mathrm{GF}[0] := \{(0,0,0)^T\} \tag{3}$$

$$\begin{aligned}\mathrm{GF}[\pm\vartheta] := \{&(\vartheta,0,0)^T,(-\vartheta,0,0)^T,(0,\vartheta,0)^T,\\&(0,-\vartheta,0)^T,(0,0,\vartheta)^T,(0,0,-\vartheta)^T\}\end{aligned} \tag{4}$$

$$\begin{aligned}\mathrm{GF}[\pm\vartheta,\pm\vartheta] := \{&(\vartheta,\vartheta,0)^T,(-\vartheta,-\vartheta,0)^T,\\&(\vartheta,-\vartheta,0)^T,(-\vartheta,\vartheta,0)^T,(\vartheta,0,\vartheta)^T,(-\vartheta,0,-\vartheta)^T,\\&(\vartheta,0,-\vartheta)^T,(-\vartheta,0,\vartheta)^T,(0,\vartheta,\vartheta)^T,(0,-\vartheta,-\vartheta)^T,\\&(0,\vartheta,-\vartheta)^T,(0,-\vartheta,\vartheta)^T\}\end{aligned} \tag{5}$$

where $\vartheta \in \mathbb{R}$ is a suitable scalar parameter. Further generator functions for arbitrary $n \in \mathbb{N}$ follow the same pattern.

Let now $g : \mathbb{R}^n \to \mathbb{R}$ be an arbitrary function and let $X = (X_1, \ldots, X_n)^T$ consist of n stochastically independent standard Gaussian components first. Then, the PEM rests upon the following approximation scheme with suitable weights $w_0, \ldots, w_m \in \mathbb{R}$ that are derived later in detail where $m \leqslant n$

$$\begin{aligned}\int_{\mathbb{R}^n} g(x)pdf_X(x)dx \approx\ & w_0 g(\mathrm{GF}[0]) + w_1 \sum g(\mathrm{GF}[\pm\vartheta])\\ &+ \cdots + w_m \sum g\Big(\mathrm{GF}\underbrace{[\pm\vartheta,\ldots,\pm\vartheta]}_{\text{m times}}\Big)\end{aligned} \tag{6}$$

The total number of sample points, thus, is given by

$$N = \sum_{j=0}^{m} 2^j \binom{n}{j} \tag{7}$$

which often is much fewer than the hundreds or thousands of sample points needed by standard MC simulations in order to converge.

The case of general distributions of X, by the way, can usually be handled with component-wise transformations of the generator functions in equation (6). For, if X_i for any $i \in \{1, \ldots, n\}$ has an arbitrary continuous distribution with a strictly monotone cumulative distribution function F_{X_i}, one obtains that $(F_{X_i}^{-1} \circ \Phi)(X_i')$ and X_i have the same distribution where X_i' is a standard Gaussian random variable with cumulative distribution function Φ. Consequently, the only thing to do with regard to applying the PEM scheme from equation (6)—which was based on the assumption of standard Gaussian random variables—is transforming each component of the original values $\xi' = (\xi_1', \ldots, \xi_n')^T$ of the generator functions (where $\xi_i' \in \{0, \vartheta, -\vartheta\}$ for all i; cf. equations (3)–(5)) via $\xi_i' \mapsto \xi_i := (F_{X_i}^{-1} \circ \Phi)(\xi_i')$ for $i = 1, \ldots, n$ before applying function g. For the reader's convenience, Table 1 explicitly lists (approximate) component-related transformations for the most common types of distributions, including some that do not have a strictly monotone distribution function.

The general PEM scheme then reads

Table 1. Transformation functions[16,18] with $\mathrm{erf}(\cdot)$ being the Gauss error function.

Distribution of X_i	Transformation function
$\mathcal{N}(\mu,\sigma)$ (Gaussian distribution)	$\xi_i = \mu + \sigma\xi_i'$
$\mathrm{Log}\mathcal{N}(\mu,\sigma)$ (Log-normal distribution)	$\xi_i = \exp(\mu + \sigma\xi_i')$
$\mathcal{U}(a,b)$ (Uniform distribution)	$\xi_i = a + (b-a)\left(\frac{1}{2} + \frac{1}{2}\mathrm{erf}\left(\xi_i'\sqrt{2}\right)\right)$
$\mathrm{Exp}(\beta)$ (Exponential distribution)	$\xi_i = -\frac{1}{\beta}\log\left(\frac{1}{2} + \frac{1}{2}\mathrm{erf}\left(\frac{\xi_i'}{\sqrt{2}}\right)\right)$
$\Gamma(\alpha,\beta)$ (Gamma distribution)	$\xi_i = \alpha\beta\left(\xi_i' \cdot \sqrt{\frac{1}{9\alpha}} + 1 - \frac{1}{9\alpha}\right)^3$
$\mathcal{W}(\beta,\eta)$ (Weibull distribution)	$\xi_i = \eta \cdot \left(-\log\left(1 - \Phi(\xi_i')\right)\right)^{1/\beta}$

$$\begin{aligned}\int_{\mathbb{R}^n} g(x)pdf_X(x)dx \approx\ & w_0 g(\tau(\mathrm{GF}[0]))\\ &+ w_1 \sum g(\tau(\mathrm{GF}[\pm\vartheta]))\\ &+ \cdots + w_m \sum g(\tau(\mathrm{GF}\underbrace{[\pm\vartheta,\ldots,\pm\vartheta]}_{\text{m times}}))\end{aligned} \tag{8}$$

where $\tau : \mathbb{R}^n \to \mathbb{R}^n$ denotes the component-wise transformation of the original generator function values as described above. Obviously, choosing $g := f$ yields the original integral from equation (1) and $g := (f - \mathbb{E}(f(X)))^2$ refers to equation (2). The remaining question is how to determine the weights w_j for $j = 0, \ldots, m$ and parameter ϑ in equations (6) and (8).

For this purpose, let $X = (X_1, \ldots, X_n)^T$ consist of n stochastically independent standard Gaussian components again (i.e. $X_i \sim \mathcal{N}(0,1)$ for $i = 1, \ldots, n$) in order to avoid the need to take account of a specific transformation as discussed above. Then, replace the general function g in equation (6) with the monomial functions $g_{i,k} : \mathbb{R}^n \to \mathbb{R}$ as defined by $g_{i,k}(x_1, \ldots, x_n) := x_i^k$ for $i = 1, \ldots, n$ and $k \in \mathbb{N} \cup \{0\}$. This finally yields the following (over-determined) system of partly (i.e. with regard to i and odd k) redundant equations as reasonable conditions for the weights $w_0, \ldots, w_m \in \mathbb{R}$ based on the corresponding raw moments of the $\mathcal{N}(0,1)$ distribution

$$\begin{aligned}&\sum_{j=0}^{m} 2^j \binom{n}{j} w_j = \int_{\mathbb{R}^n} 1 pdf_X(x)dx \text{ and}\\ &\left(\vartheta^k + (-\vartheta)^k\right)\sum_{j=1}^{m} 2^{j-1}\binom{n-1}{j-1}w_j\\ &= \int_{\mathbb{R}^n} x_i^k pdf_X(x)dx \ \ (\text{for all } k > 0)\end{aligned} \tag{9}$$

Taking only the first three raw moments into account (i.e. $k = 0,\ 1,\ 2,\ 3$) and choosing $m = 1$, equation (9) becomes

$$w_0 + 2nw_1 = 1 \ \text{ and } \ 2\vartheta^2 w_1 = 1 \tag{10}$$

after the elimination of all redundancies. The resulting PEM scheme (cf. equation (6)) reads

$$\int_{\mathbb{R}^n} g(x)pdf_X(x)dx \approx \left(1-\frac{n}{\vartheta^2}\right)g(\mathrm{GF}[0]) + \frac{1}{2\vartheta^2}\sum g(\mathrm{GF}[\pm\vartheta]) \tag{11}$$

Note that the corresponding scheme for arbitrary distributions of X (cf. equation (8)) uses the same weights. For some reason,[16] by the way, a common value of the remaining parameter is $\vartheta = \sqrt{3}$. Moreover, it can be shown easily that the scheme from equation (11) is exact whenever the function g is a polynomial of degree not greater than 3. The same naturally holds for the more general scheme with the additional transformation $\tau : \mathbb{R}^n \to \mathbb{R}^n$ if the composite function $g \circ \tau$ has such a form in this case.

In order to increase the accuracy of the PEM for polynomials of higher degrees, one may choose larger values of k and m, but at the cost of additional sample points that need to be evaluated, of course. Consider the first five raw moments in equation (9), for instance, where $m = 2$. Moreover, in order to finally guarantee exact precision for polynomials of degree not greater than 5, join further equations based on the non-monomial functions $g_{i,2|l,2} : \mathbb{R}^n \to \mathbb{R}$ with $g_{i,2|l,2}(x_1, \ldots, x_n) := x_i^2 x_l^2$ for $i, l = 1, \ldots, n$ and $i \neq l$ to the conditions from equation (9) when determining the corresponding weights w_0, w_1 and w_2 as well as parameter ϑ. Namely

$$4\vartheta^4 w_2 = \int_{\mathbb{R}^n} x_i^2 x_l^2 pdf_X(x)dx = 1 \tag{12}$$

for stochastically independent $X_i \sim \mathcal{N}(0,1)$ and $X_l \sim \mathcal{N}(0,1)$. The resulting (improved) PEM scheme for standard Gaussian inputs X then reads

$$\int_{\mathbb{R}^n} g(x)pdf_X(x)dx \approx \left(1+\frac{n^2-7n}{18}\right)g(\mathrm{GF}[0]) + \frac{4-n}{18}\sum g(\mathrm{GF}[\pm\vartheta]) + \frac{1}{36}\sum g(\mathrm{GF}[\pm\vartheta,\pm\vartheta]) \tag{13}$$

where necessarily $\vartheta = \sqrt{3}$.

As already suggested, this scheme is exact up to polynomials of degree not greater than 5. That is, whenever the function g or $g \circ \tau$, respectively, is well-approximated by such a polynomial, the PEM can be expected to provide highly accurate results. However, it is very difficult to say in advance how well the PEM performs when g or $g \circ \tau$ become more complex. The section "Applications", therefore, discusses some of these examples using the PEM scheme from equation (13) as default.

In this context, the PEM becomes a simple step-by-step procedure that can easily be applied to nearly any given model f with input variables given by the vector $X = (X_1, \ldots, X_n)^T$. Here, n is the number of uncertain input variables with distributions that are expected to be known. With regard to the model response $Y = f(X)$, the PEM workflow (cf. Figure 1) reads as follows:

i. Make a list of the n-dimensional tuples $\xi' = (\xi'_1, \ldots, \xi'_n)^T$ based on the pattern from equations (3) to (5) where $\vartheta = \sqrt{3}$.
ii. Compute the actual PEM sample by element-wise transformations of the tuples from step (i) using Table 1. This results in a set of transformed tuples $\xi = (\xi_1, \ldots, \xi_n)^T$. (Note that in case of standard Gaussian components such a transformation is not necessary.)
iii. Depending on the quantity of interest, choose one of the following functions g for the further computations:
   (a) For $\mathbb{E}(Y)$ (=mean), consider the function $g : \xi \mapsto f(\xi)$
   (b) For $\mathbb{E}(Y^2)$ (=second moment), consider the function $g : \xi \mapsto f(\xi)^2$
   (c) For $\mathrm{Var}(Y)$ (=variance), consider the function $g : \xi \mapsto (f(\xi) - \mathbb{E}(Y))^2$ where $\mathbb{E}(Y)$ is the previously derived PEM estimate for the mean using the function from step (iii-a). (Note that the variance can also be computed via $\mathrm{Var}(Y) = \mathbb{E}(Y^2) - (\mathbb{E}(Y))^2$ where $\mathbb{E}(Y)$ and $\mathbb{E}(Y^2)$ are the PEM estimates for the mean and the second moment using the functions from step (iii-a and b.))
   (d) For $\mathbb{E}(Y^k)$ (=kth moment), consider the function $g : \xi \mapsto f(\xi)^k$.

   (Note that other statistical quantities are possible as well. Each one corresponds to a specific definition of the function g in the PEM scheme from equation (13).)
iv. Compute the model response values using the function g from step (iii) based on the transformed tuples $\xi = (\xi_1, \ldots, \xi_n)^T$ from step (ii).
v. Compute the weighted sum according to the PEM scheme from equation (13) based on the specific model response values from step (iv) which yields the PEM estimate for the quantity of interest.

Applications

Railway asset management usually requires tools for monitoring and predicting the health states of the rail infrastructure. These tools can rely on physical (i.e. model-based) and/or statistical (i.e. data-driven) approaches, for instance.[1] Moreover, causes of failure need to be identified effectively (diagnosis) in order to optimize maintenance processes whenever malfunctions occur.

Track degradation

Regarding railway track sections, Andrews and colleagues[19,20] proposed a quite complex Petri net model

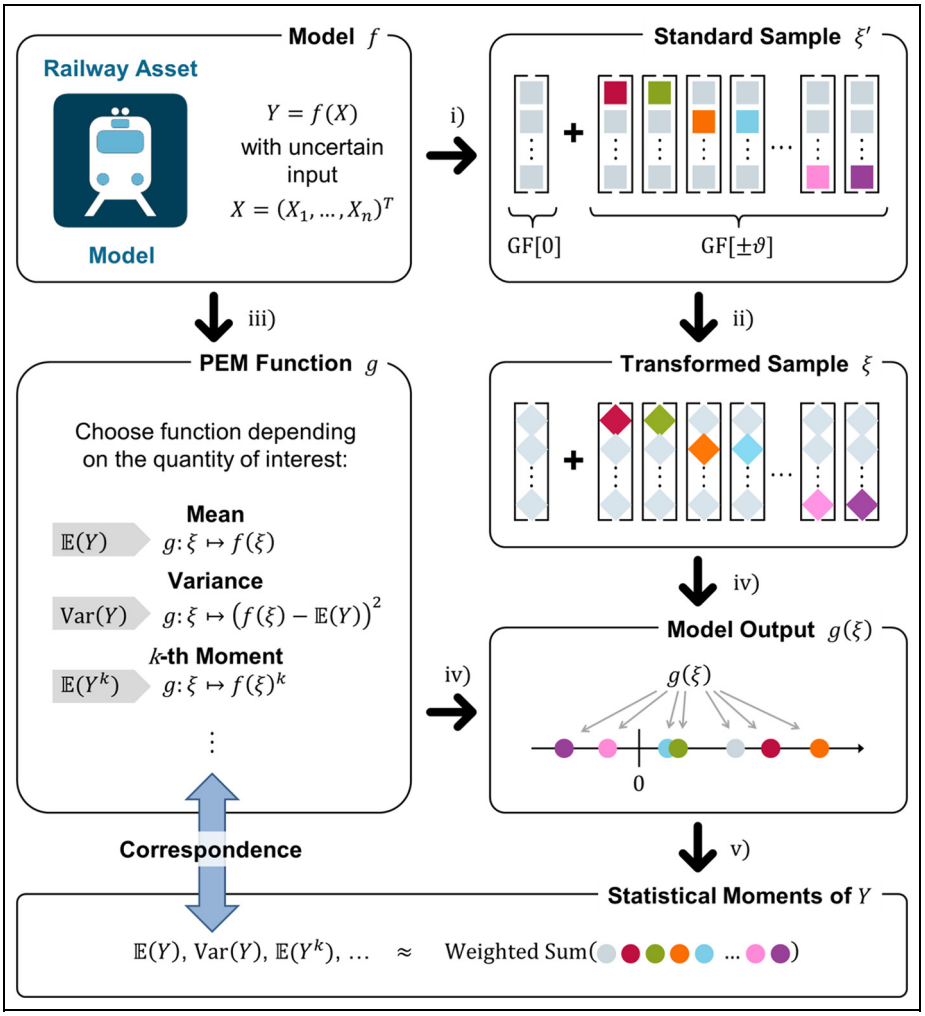

Figure 1. Work-flow of the PEM (exemplarily shown for the case $m = 1$).

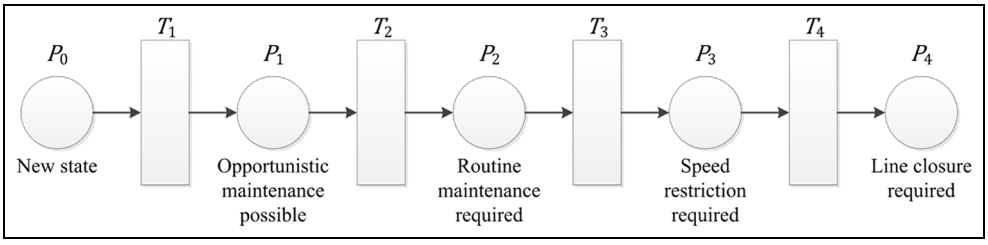

Figure 2. Petri net model for track degradation.[19]

for simulating the interaction between all relevant processes in track asset management. Their model includes parts for deterioration, inspection, intervention, and renewal. A similar Petri net model, by the way, is available for bridge maintenance,[21] for instance. Figure 2 shows the degradation part of the model in an extended version with five instead of four health states (i.e. $P_0, \ldots, P_4$). In this context, the transitions $T_1, \ldots, T_4$ describe the durations in time (in days) after which the system switches to the corresponding next health state. They are considered to be stochastically independent random variables having Weibull distributions

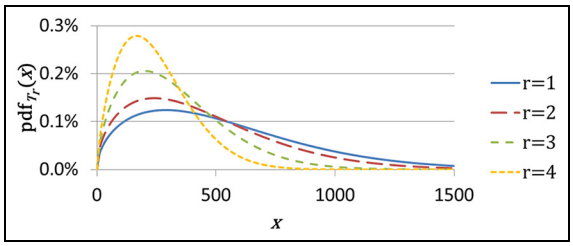

Figure 3. Probability density functions of the transition times T_r.

Table 2. Expert guess of the Weibull parameters of the degradation model.[22]

	T_1	T_2	T_3	T_4
β_r (shape)	1.5	1.5	1.6	1.7
η_r (scale)	600	500	370	280

$\mathcal{W}(\beta_r, \eta_r)$ for $r = 1, \ldots, 4$ (see Figure 3) with parameters as in Table 2.

Starting from state P_0 (i.e. directly after renewal or new construction), the duration before the system reaches the state P_s for $s = 1, \ldots, 4$ is defined then by

$$\tilde{T}_s := \sum_{r=1}^{s} T_r \tag{14}$$

Thus, the expectation and standard deviation of $\tilde{T}_s$ (in days) are given by

$$\mathbb{E}(\tilde{T}_s) = \sum_{r=1}^{s} \mathbb{E}(T_r) = \sum_{r=1}^{s} \eta_r \Gamma\left(1 + \frac{1}{\beta_r}\right) \tag{15}$$

and

$$\begin{aligned} \sigma(\tilde{T}_s) &= \mathrm{Var}(\tilde{T}_s)^{\frac{1}{2}} = \left(\sum_{r=1}^{s} \mathrm{Var}(T_r)\right)^{\frac{1}{2}} \\ &= \left(\sum_{r=1}^{s} \eta_r^2 \left[\Gamma\left(1 + \frac{2}{\beta_r}\right) - \left(\Gamma\left(1 + \frac{1}{\beta_r}\right)\right)^2\right]\right)^{\frac{1}{2}} \end{aligned} \tag{16}$$

In comparison with these analytical solutions, Table 3 shows the numerical results obtained by standard MC simulations with 10,000 samples and PEM approximations using equation (13) for $\mathbb{E}(\tilde{T}_s)$ and $\mathrm{Var}(\tilde{T}_s)$ with an additional application of the transformation for Weibull distributions from Table 1. The corresponding relative errors Δ_{rel} referring to the exact (i.e. analytical) values from equations (15) and (16) are given in Table 4.

The full (approximate) distributions of $\tilde{T}_s$ for $s = 1, \ldots, 4$—as derived from the MC simulations—are depicted in Figure 4(a) in the form of the corresponding reliability functions $t \mapsto R_{\tilde{T}_s}(t) := 1 - F_{\tilde{T}_s}(t)$ where $F_{\tilde{T}_s}$ is the cumulative distribution function of $\tilde{T}_s$. Moreover, Figure 4(b) shows the simulated probabilities for the states $P_0, \ldots, P_4$ depending on the time since renewal.

As can be seen, the PEM and the MC simulations both provide good results for the degradation model. In fact, the PEM approximations are even nearly exact (cf. Tables 3 and 4) which is not that surprising in this case because $\tilde{T}_s$ is a simple linear combination of the input variables T_r. Moreover, the function $(\tilde{T}_s - \mathbb{E}(\tilde{T}_s))^2$ which is used for computing the variances via the PEM is quadratic then. Consequently, as the PEM scheme from equation (13) is exact for polynomials of degree not greater than 5, the only source of error results from the (more or less) exact Weibull transformation in Table 1. In contrast, the MC approach shows relative errors up to $\pm 1\%$ despite a large sample size (i.e. 10,000 evaluations). This result is quite striking when noting that the (nearly exact) PEM in this case requires 33 distinguished sample points only. Effectively, even just 25 (!) sample points need to be considered because the second weight in equation (13) equals zero when $n = 4$. However, note that the PEM is not directly able to reconstruct the full distributions of $\tilde{T}_s$ in Figure 4. Because of its small sample size, the direct empirical computation of the cumulative distribution functions analogously to the MC approach is not possible with sufficient quality. That is, the model response for $\tilde{T}_s$, for instance, takes merely 33 (or even fewer) different discrete values in case of the PEM sampling while the true distributions are continuous. Consequently, the PEM usually provides statistical moments (e.g. mean or variance) only. Of course, if the shape of the output distribution is known in some rare situations, the

Table 3. Comparison of the results for $\mathbb{E}(\tilde{T}_s)$ and $\sigma(\tilde{T}_s)$ (in days).

	$\mathbb{E}(\tilde{T}_1)$	$\sigma(\tilde{T}_1)$	$\mathbb{E}(\tilde{T}_2)$	$\sigma(\tilde{T}_2)$	$\mathbb{E}(\tilde{T}_3)$	$\sigma(\tilde{T}_3)$	$\mathbb{E}(\tilde{T}_4)$	$\sigma(\tilde{T}_4)$
Analytical	541.6	367.8	993.0	478.7	1324.8	523.7	1574.6	545.1
MC	538.0	369.6	983.1	478.6	1317.3	526.3	1566.8	548.7
PEM	541.7	367.6	993.1	478.6	1324.8	523.4	1574.7	544.7

MC: Monte Carlo; PEM: point estimate method.

Table 4. Relative errors of the MC approach and PEM for $\mathbb{E}(\tilde{T}_s)$ and $\sigma(\tilde{T}_s)$.

Δ_{rel}	$\mathbb{E}(\tilde{T}_1)$	$\sigma(\tilde{T}_1)$	$\mathbb{E}(\tilde{T}_2)$	$\sigma(\tilde{T}_2)$	$\mathbb{E}(\tilde{T}_3)$	$\sigma(\tilde{T}_3)$	$\mathbb{E}(\tilde{T}_4)$	$\sigma(\tilde{T}_4)$
MC	−0.68%	+0.50%	−1.00%	−0.03%	−0.56%	+0.50%	−0.49%	+0.67%
PEM	+0.00%	−0.03%	+0.00%	−0.03%	+0.01%	−0.05%	+0.01%	−0.07%

MC: Monte Carlo; PEM: point estimate method.

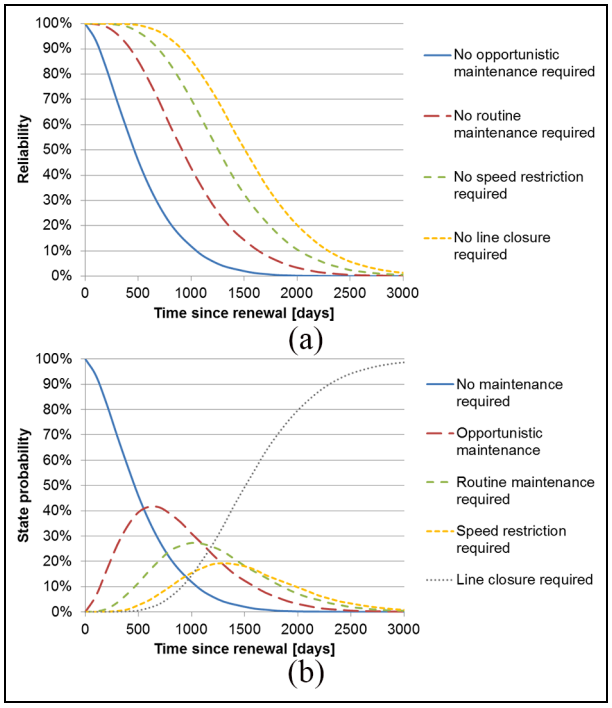

Figure 4. (a) Simulated track reliability with regard to the modeled degradation levels and (b) simulated state probabilities depending on time since renewal in days.

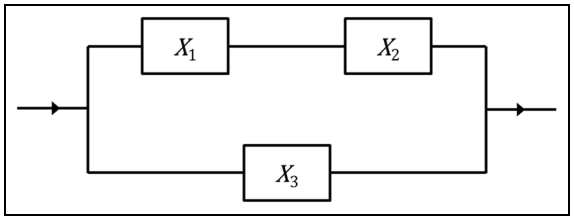

Figure 5. Structure of the analyzed composite system.

statistical moments computed by the PEM might be used to estimate the full distribution via common statistical techniques nonetheless.

Reliability of composite systems

Rail infrastructures are commonly characterized by a complex interaction of many elements (e.g. tracks, signaling, switches, and crossings). Moreover, note that each such element can be composed of several redundant and/or non-redundant components itself. Consequently, assessing reliability in this context naturally means also to analyze composite systems instead of single components only. As a simple generic example, consider a (technical) system that consists of three independent components X_1, X_2, X_3 each having an exponential life distribution, that is, $X_i \sim \text{Exp}(\beta_i)$ with scale parameters $\beta_i > 0$ for $i = 1, 2, 3$. Let the first two components (X_1, X_2) be connected in series, while the third component (X_3) is connected in parallel (cf. Figure 5). The system is considered as ready for service whenever all components of at least one of the branches in Figure 5 are available.

In reliability theory,[23] it is common then—similar to the previous degradation example—to ask for the probability that the considered system *survives* until time t. In this context, the survival functions $R_{X_i} : [0, \infty) \to \mathbb{R}$ for the single components are defined by

$$R_{X_i}(t) := 1 - F_{X_i}(t) = \exp\left(-\frac{t}{\beta_i}\right) \tag{17}$$

where $F_{X_i} : [0, \infty) \to \mathbb{R}$ for $i = 1, 2, 3$ is the cumulative distribution function of X_i. Moreover, the system survival function $R_{\text{sys}} : [0, \infty) \to \mathbb{R}$ can be derived easily[23] from the system structure in Figure 5 because of the assumption of independent X_i. Namely

$$\begin{aligned} R_{\text{sys}}(t) &= 1 - (1 - R_{X_1}(t)R_{X_2}(t))(1 - R_{X_3}(t)) \\ &= R_{X_1}(t)R_{X_2}(t) + R_{X_3}(t) - R_{X_1}(t)R_{X_2}(t)R_{X_3}(t) \end{aligned} \tag{18}$$

Obviously, this is a deterministic function given fixed scale parameters β_i for $i = 1, 2, 3$. From an uncertainty perspective, however, β_i for $i = 1, 2, 3$ in equation (17) usually (i.e. for most practical purposes) is an estimated value only and thus must finally be considered a random variable as well. In such a way, $R_{\text{sys}}(t)$ as defined in equation (18)—for each $t \geqslant 0$—corresponds to function f in the description of the PEM above with the probabilistic input vector $(\beta_1, \beta_2, \beta_3)^T$. In order to demonstrate that the PEM really is able to cope with various combinations of input distributions, the following (artificial) assumptions on the variables β_i for $i = 1, 2, 3$ were made

$$\beta_1 \sim \Gamma(2, 0.5) \quad (\text{Gamma distribution}) \tag{19}$$

$$\beta_2 \sim \mathcal{U}(1, 3) \quad (\text{Uniform distribution}) \tag{20}$$

$$\beta_3 \sim \text{Log}\mathcal{N}(1, 0.4) \quad (\text{Log} - \text{normal distribution}) \tag{21}$$

Figure 6 shows the corresponding probability density functions of $\beta_1, \beta_2, \beta_3$. The expected value and variance of $\beta_1, \beta_2, \beta_3$ are given by $\mathbb{E}(\beta_1) = 4$ and $\text{Var}(\beta_1) = 8$; $\mathbb{E}(\beta_2) = 2$ and $\text{Var}(\beta_2) = 0.3333$; $\mathbb{E}(\beta_3) = 2.9447$ and $\text{Var}(\beta_3) = 1.5045$.

Applying the PEM scheme from equation (13) to the function $R_{\text{sys}}(t)$ with uncertain β_i, together with the appropriate transformations from Table 1, yields approximate values of $\mathbb{E}(R_{\text{sys}}(t))$ as well as $\text{Var}(R_{\text{sys}}(t))$ for any given t. Figure 7 depicts these PEM results—computed for several values of t—as a time series where standard MC simulations were performed as reference.

As can be seen, the PEM is able to provide highly accurate estimates for $\mathbb{E}(R_{\text{sys}}(t))$ and $\text{Var}(R_{\text{sys}}(t))$ in this example while requiring only 19 (!) sample points to be evaluated per value of t. In contrast to that, the MC results are based on the evaluation of 10,000 sample points per value of t as in previous examples. In other

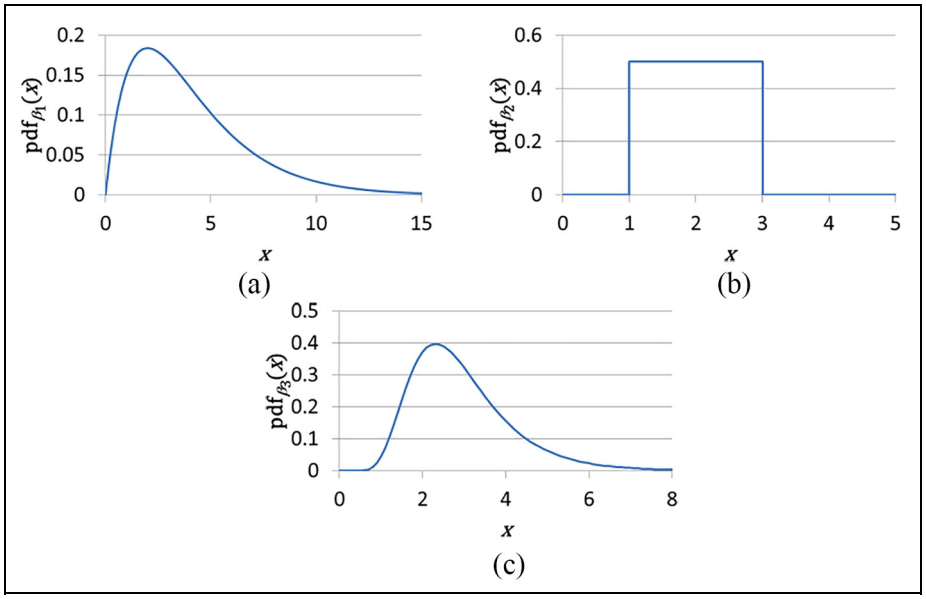

Figure 6. Probability density functions of the input parameter distributions: (a) $\beta_1 \sim \Gamma(2, 0.5)$, (b) $\beta_2 \sim \mathcal{U}(1, 3)$, and (c) $\beta_3 \sim \text{Log}\mathcal{N}(1, 0.4)$.

words, the uncertainty of $R_{\text{sys}}(t)$—depending on the distributions of the input parameters $\beta_1, \beta_2, \beta_3$—is figured out very well by the PEM. It seems that (also after the transformation according to Table 1) the non-polynomial function $R_{\text{sys}}(t)$ from equation (18) is sufficiently approximated by a polynomial with a degree not greater than 5 for which the PEM scheme from equation (13) would provide even exact results.

Terminal reliability in rail networks

The concept of system reliability, which is based on the analysis of corresponding survival functions as in the previous example, is not only relevant to technical elements but can also be applied to study the availability of operational connections between given locations in transportation networks (i.e. terminal reliability[24]) when links randomly fail. Fecarotti,[10] for instance, used such a system reliability approach in the context of optimizing maintenance strategies for railway networks in order to take account of the effect that maintenance-induced temporary link closures have on the overall network connectivity.

As a simple example, consider the rail network from Figure 8 and ask for the reliability of the connection between the stations A and B when the links degrade according to the Petri net model from Figure 2. In other words, how likely is it that there is a connection available at time t when every single link may fail (i.e. requires to be closed) due to degradation as modeled previously in the first presented example (see section "Track degradation")?

According to equation (14), the survival time $\tilde{T}^{(i)}$ of link X_i is the sum of four Weibull variables. For the sake of simplicity, however, assume that it is a Weibull variable directly; that is, $\tilde{T}^{(i)} \sim \mathcal{W}(\beta^{(i)}, \eta^{(i)})$ for $i = 1, \ldots, 6$. The parameters $\beta^{(i)}$ and $\eta^{(i)}$ are defined via a maximum likelihood estimation in a first step based

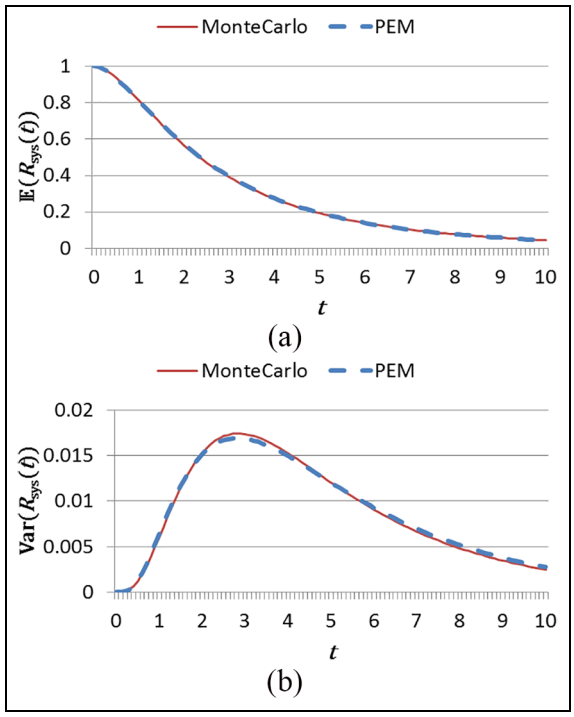

Figure 7. PEM results in comparison with standard MC simulations: (a) $\mathbb{E}(R_{\text{sys}}(t))$ and (b) $\text{Var}(R_{\text{sys}}(t))$.

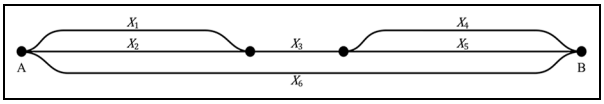

Figure 8. A simple rail network.

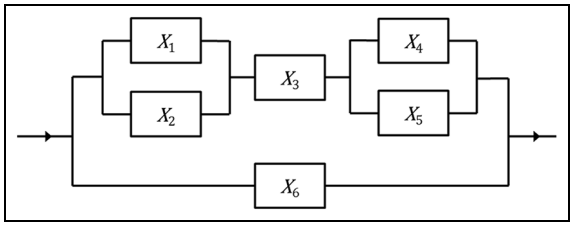

Figure 9. Block diagram representation of the rail network from Figure 8.

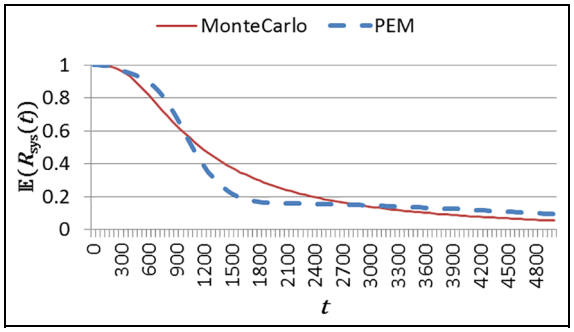

Figure 10. Expected network reliability in case of Weibull distributed survival times per link (i.e. $\beta^{(i)} = 3.035$).

on simulated random samples of $\tilde{T}^{(i)}$ using the original model from Figure 2. This results in $\beta^{(i)} = 3.035$ and $\eta^{(i)} = 1754.2$ which—in good agreement with Table 3—corresponds to a mean survival time of $\mathbb{E}(\tilde{T}^{(i)}) = 1567.3$ (in days) for all $i = 1, \ldots, 6$. Note that degradation characteristics may differ from one link to another, of course, meaning that the Weibull parameters above are typically uncertain to some extent. In particular, the scale parameters $\eta^{(i)}$ can be expected to vary considerably among the links, while $\beta^{(i)}$ for $i = 1, \ldots, 6$ is finally considered as deterministic. In the following, the parameters $\eta^{(i)}$ for $i = 1, \ldots, 6$ are modeled as stochastically independent and identically distributed Log-normal random variables. Note that even if there is no specific (i.e. empirically motivated) reason for choosing this type of distribution for $\eta^{(i)}$ in this academic example, the Log-normal distribution—instead of a Gaussian distribution, for instance—ensures that $\eta^{(i)}$ never gets negative and thus $\mathcal{W}(\beta^{(i)}, \eta^{(i)})$ always is a valid distribution for $\tilde{T}^{(i)}$. More precisely, let $\eta^{(i)} \sim \mathrm{Log}\mathcal{N}(\mu, \sigma)$ with $\mu = 6.96977$ and $\sigma = 1.0$ which means that the expectation of the survival time $\tilde{T}^{(i)}$ remains the same as before despite the additional stochasticity of $\eta^{(i)}$. In fact

$$\begin{aligned}\mathbb{E}\left(\tilde{T}^{(i)}\right) &= \mathbb{E}\left(\eta^{(i)} \cdot \Gamma\left(1 + \frac{1}{\beta^{(i)}}\right)\right) \\ &= \mathbb{E}\left(\eta^{(i)}\right) \cdot \Gamma\left(1 + \frac{1}{\beta^{(i)}}\right) = 1567.3 \quad \text{(in days)}\end{aligned} \tag{22}$$

for all $i = 1, \ldots, 6$.

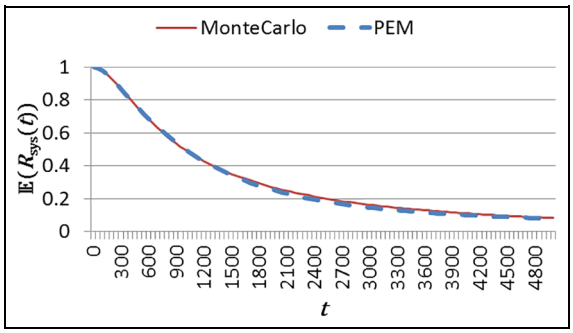

Figure 11. Expected network reliability in case of exponentially distributed survival times per link (i.e. $\beta^{(i)} = 1$).

Because of $\tilde{T}^{(i)} \sim \mathcal{W}(\beta^{(i)}, \eta^{(i)})$ for $i = 1, \ldots, 6$, the survival functions $R_{X_i} : [0, \infty) \to \mathbb{R}$ for the links $X_1, \ldots, X_6$ are given as time-dependent random variables according to

$$R_{X_i}(t) = \exp\left(-\left(\frac{t}{\eta^{(i)}}\right)^{\beta^{(i)}}\right) \tag{23}$$

Furthermore, the system survival function $R_{\mathrm{sys}} : [0, \infty) \to \mathbb{R}$, which corresponds to the rail network from Figure 8, reads

$$R_{\mathrm{sys}}(t) = 1 - (1 - R_{X_1X_2X_3X_4X_5}(t)) \cdot (1 - R_{X_6}(t)) \tag{24}$$

with

$$R_{X_1X_2X_3X_4X_5}(t) := R_{X_1X_2}(t) \cdot R_{X_3}(t) \cdot R_{X_4X_5}(t) \tag{25}$$

and

$$R_{X_1X_2}(t) := R_{X_1}(t) + R_{X_2}(t) - R_{X_1}(t)R_{X_2}(t) \tag{26}$$

$$R_{X_4X_5}(t) := R_{X_4}(t) + R_{X_5}(t) - R_{X_4}(t)R_{X_5}(t) \tag{27}$$

In this context, note that the network from Figure 8 can also be depicted as a standard block diagram (see Figure 9).

Estimates of $\mathbb{E}(R_{\mathrm{sys}}(t))$ are finally derived by using the PEM based on 73 sample points and MC simulations with 10,000 sample points for each considered value of t. Figure 10 shows the results. As can be seen, the PEM does not provide sufficiently accurate results in this case even if the asymptotic trends of the depicted curves have some similarity.

It turns out that the lack of accuracy is mostly because of the non-polynomial structure of the survival functions from equation (23) which is induced by the shape parameters $\beta^{(i)} \neq 1$. If, for instance, $\beta^{(i)} = 1$ for all $i = 1, \ldots, 6$, the PEM results become much better. In fact, there is hardly any difference between the estimates as generated by the PEM and the MC simulations in that situation (see Figure 11). Obviously, exponentially distributed survival times $\tilde{T}^{(i)}$ with $\beta^{(i)} = 1$ (instead of Weibull distributions with $\beta^{(i)} \neq 1$) are more accessible for polynomial approximations which turns out to be a crucial requirement for

Table 5. Conditional distributions of the feature values X_1, X_2, X_3.

$\mathbb{P}(X_i \mid Z = z_j)$	X_1	X_2	X_3
$Z = z_0$ (No failure)	$\mathcal{N}(0.6, 0.1)$	$\mathcal{N}(0.5, 0.12)$	$\mathcal{N}(0.7, 0.1)$
$Z = z_1$ (Failure type 1)	$\mathcal{N}(0.6, 0.1)$	$\mathcal{N}(0.5, 0.12)$	$\mathcal{N}(0.35, 0.05)$
$Z = z_2$ (Failure type 2)	$\mathcal{N}(0.35, 0.1)$	$\mathcal{N}(0.35, 0.1)$	$\mathcal{N}(0.4, 0.08)$

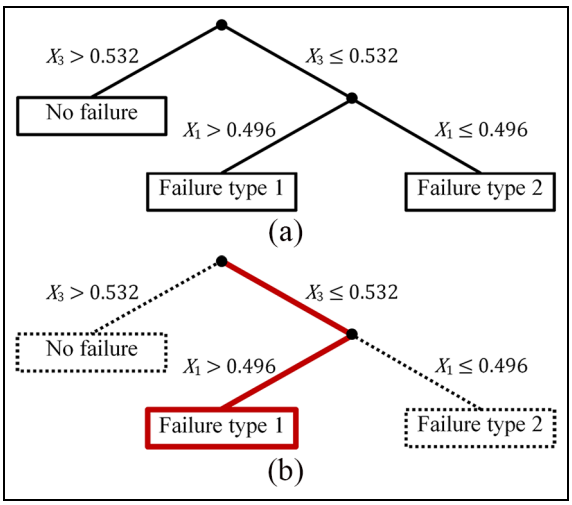

Figure 12. (a) Decision tree model and (b) relevant branch in the case of $X_1 = 0.65$, $X_2 = 0.5$, and $X_3 = 0.3$.

obtaining highly accurate PEM results based on the scheme from equation (13).

Failure mode identification using decision trees

Consider a technical system or component—this could be a track element or a switch component, for instance—that usually adopts one of the following three possible operating states Z: "No failure" (z_0), "Failure type 1" (z_1), or "Failure type 2" (z_2). Assume further that the system is monitored based on three (conditionally) independent feature values X_1, X_2, X_3 having Gaussian (conditional) distributions given Z as listed in Table 5.

It is possible then to derive a suitable decision tree (model) for identifying the operating states from (measured) feature values. Applications and discussions of decision tree modeling in the context of railway asset management, for instance, can be found in the literature.[13,25,26] With regard to the features and distributions from Table 5, Figure 12(a) shows the decision tree that was automatically built from an artificial training data set using state-of-the-art algorithms.[27] Given the realization of the three feature values X_1, X_2, X_3, a corresponding estimate of the operating state is easily obtained by simply finding the related branch in the decision tree. Figure 12(b), for instance, shows this branch for a virtual measurement, where $X_1 = 0.65$, $X_2 = 0.5$, and $X_3 = 0.3$. Obviously, the model yields "Failure type 1" as result in this case.

The question is how likely the diagnostic outcome of the model is correct. That is, what is the uncertainty in the model output? For this purpose, let

$$f(X_1, X_2, X_3) = \begin{pmatrix} f_0(X_1, X_2, X_3) \\ f_1(X_1, X_2, X_3) \\ f_2(X_1, X_2, X_3) \end{pmatrix} := \begin{pmatrix} \mathbb{1}_{\{X_3 > 0.532\}} \\ \mathbb{1}_{\{X_1 > 0.496\}} \cdot \mathbb{1}_{\{X_3 \leq 0.532\}} \\ \mathbb{1}_{\{X_1 \leq 0.496\}} \cdot \mathbb{1}_{\{X_3 \leq 0.532\}} \end{pmatrix} \tag{28}$$

be the formula-based representation of the decision tree model from Figure 12(a) where $f_i : \mathbb{R} \to \{0, 1\}$ for $i = 0, 1, 2$ is the indicator function whether the model "predicts" z_i as operating state (i.e. $f_i(X_1, X_2, X_3) = 1$) or not (i.e. $f_i(X_1, X_2, X_3) = 0$).

As now X_1, X_2, X_3 are random variables given Z, one directly obtains that $f_i(X_1, X_2, X_3)$ for $i = 1, 2, 3$ are random variables as well. More precisely

$$\mathbb{P}\big(f_i(X_1, X_2, X_3) \mid Z = z_j\big) = \mathcal{B}\big(1, p_{ij}\big) \tag{29}$$

for all $i, j = 0, 1, 2$ with unknown parameters $p_{ij} \in [0,\ 1]$ for the appearing Bernoulli distributions $\mathcal{B}(1, p)$. Thus, p_{ij} is the probability that the decision tree model from Figure 12(a) yields the operating state z_i given that the true operating state is z_j. Moreover, for all $j = 0, 1, 2$, the expected value and variance of $f(X_1, X_2, X_3)$ given $Z = z_j$ are finally defined by

$$\mathbb{E}\big(f(X_1, X_2, X_3) \mid Z = z_j\big) = \begin{pmatrix} \mathbb{E}\big(f_0(X_1, X_2, X_3) \mid Z = z_j\big) \\ \mathbb{E}\big(f_1(X_1, X_2, X_3) \mid Z = z_j\big) \\ \mathbb{E}\big(f_2(X_1, X_2, X_3) \mid Z = z_j\big) \end{pmatrix} = \begin{pmatrix} p_{0j} \\ p_{1j} \\ p_{2j} \end{pmatrix} \tag{30}$$

and

$$\mathrm{Var}\big(f(X_1, X_2, X_3) \mid Z = z_j\big) = \begin{pmatrix} \mathrm{Var}\big(f_0(X_1, X_2, X_3) \mid Z = z_j\big) \\ \mathrm{Var}\big(f_1(X_1, X_2, X_3) \mid Z = z_j\big) \\ \mathrm{Var}\big(f_2(X_1, X_2, X_3) \mid Z = z_j\big) \end{pmatrix} = \begin{pmatrix} p_{0j}\big(1 - p_{0j}\big) \\ p_{1j}\big(1 - p_{1j}\big) \\ p_{2j}\big(1 - p_{2j}\big) \end{pmatrix} \tag{31}$$

respectively.

Needless to say, it is very easy then to apply the PEM scheme from equation (13) together with the

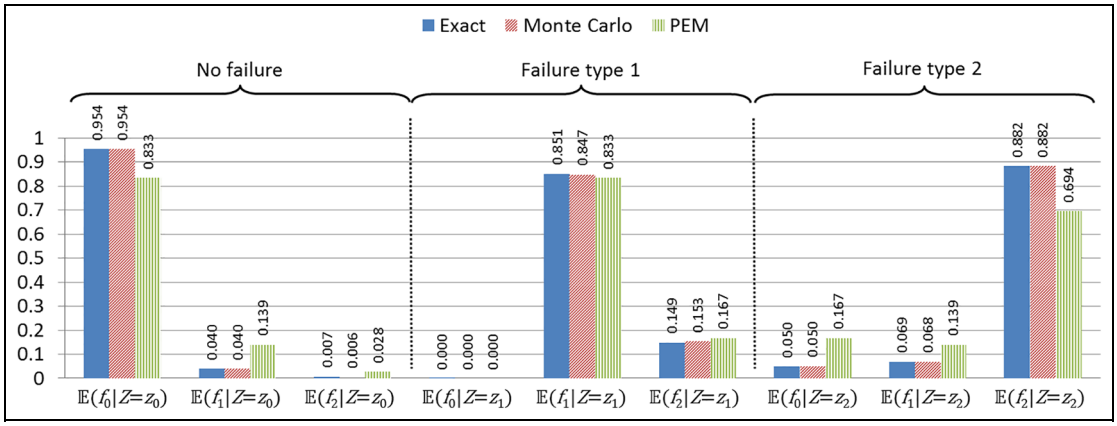

Figure 13. Comparison of the results for $\mathbb{E}(f(X_1, X_2, X_3)|Z = z_j)$.

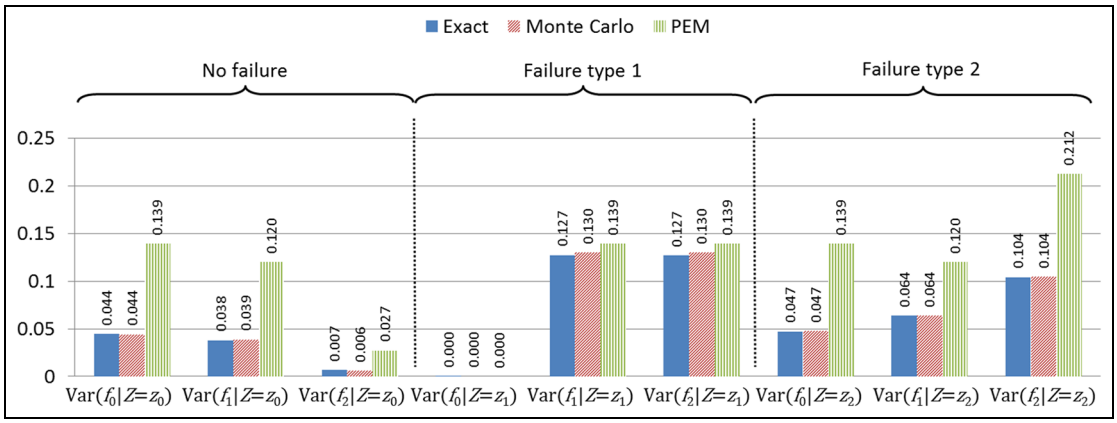

Figure 14. Comparison of the results for $\mathrm{Var}(f(X_1, X_2, X_3)|Z = z_j)$.

appropriate transformations from Table 1 in order to compute explicit estimates for the unknown values in equations (30) and (31). The only thing one has to be careful with is that the input variables X_1, X_2, X_3 have different (conditional) distributions depending on the current operating state (see Table 5). Figure 13 shows the resulting estimates for $\mathbb{E}(f(X_1, X_2, X_3)|Z = z_j)$ in comparison with MC simulations, as well as exact results which are obtained by directly solving the conditional equations

$$\mathbb{P}\big(f_i(X_1, X_2, X_3) = 1|Z = z_j\big) = p_{ij} \tag{32}$$

for p_{ij} where $i, j = 0, 1, 2$ (see Appendix 1). The estimates for $\mathrm{Var}(f(X_1, X_2, X_3)|Z = z_j)$ are displayed in Figure 14.

As can be seen, the PEM yields almost correct trends for all the values in equations (30) and (31). That is, whenever $\mathbb{E}(f_i(X_1, X_2, X_3)|Z = z_j)$ or $\mathrm{Var}(f_i(X_1, X_2, X_3)|Z = z_j)$ attains its maximum for any fixed j, the PEM yields the highest value among all i, too. The bar charts in Figures 13 and 14, however, also imply that the accuracy of the PEM is much lower than that of the MC approach in this example. Obviously, the discontinuity and step structure of the model function f from equation (28) (which, of course, is far from being polynomial) prevent the PEM from generating sufficiently accurate results. Consequently, in contrast to the previous examples, the PEM turns out to be not well-suited for analyzing uncertainty propagation in the case of decision tree models as in Figure 12.

Track condition modeling incorporating maintenance

Consider a track section that deteriorates according to the degradation model as given in Figure 2. Furthermore, assume that maintenance (e.g. tamping) brings the track conditions back to the (new) state P_0 whenever a specific health state P_i with $i \geqslant 1$ is detected (and repaired) before the track section degrades to the next worse state. The extended model with added transitions M_r for $r = 1, \ldots, 4$ (see Figure 15) is very similar to the original Petri net presented by Andrews and colleagues.[19,20] Although, for simplicity, it does not consider that the degradation parameters of the track section may change after each maintenance intervention.[28]

Note that every M_r in the proposed model is composed of a random time D_r until the health state P_r (if

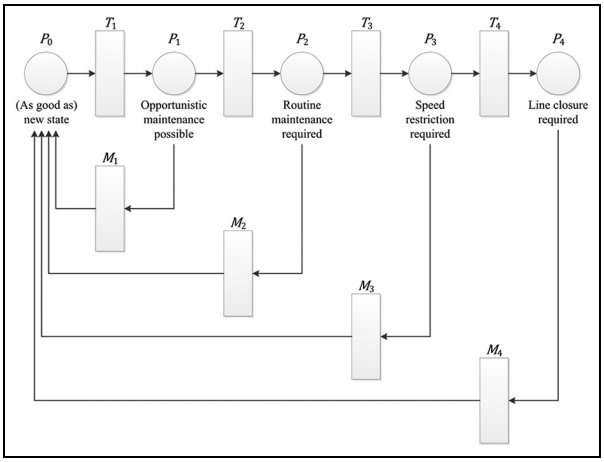

Figure 15. Extended Petri net model for track degradation incorporating maintenance.

present) is detected via inspection and the related stochastic repair time R_r. In other words, $M_r = D_r + R_r$ for $r = 1, \ldots, 4$ where the repair times also include a certain potential of postponing the related maintenance interventions depending on their urgency. In case of state P_1, for instance, that means that the values of $\mathbb{E}(R_1)$ and $\mathrm{Var}(R_1)$ may be very different from those related to the other health states because of a much lower priority of opportunistic maintenance compared to routine or even emergency interventions. Given that there is a fixed inspection interval T_{inspect}, the detection delays D_r can be modeled then as (independent) uniformly distributed random variables for all r, namely, $D_r \sim \mathcal{U}(0, T_{\text{inspect}})$. Moreover, repair times are considered having Log-normal distributions with parameters as in Table 6, that is, $R_r \sim \mathrm{Log}\mathcal{N}(\mu_r, \sigma_r)$ for $r = 1, \ldots, 4$. Table 7 lists the corresponding mean repair times and their standard deviations, respectively.

Based on this model, an asset manager could now be interested in the expected time of sojourning in a state that requires line restrictions (i.e. speed restriction or line closure) between two maintenance interventions. Thus, consider the related functions

$$T_{\text{Speed Restriction}} := \mathbb{1}_{\{M_1 \geq T_2\}} \cdot \mathbb{1}_{\{M_2 \geq T_3\}} \cdot \left(\mathbb{1}_{\{M_3 < T_4\}} \cdot M_3 + \mathbb{1}_{\{M_3 \geq T_4\}} \cdot T_4\right) \tag{33}$$

and

$$T_{\text{Line Closure}} := \mathbb{1}_{\{M_1 \geq T_2\}} \cdot \mathbb{1}_{\{M_2 \geq T_3\}} \cdot \mathbb{1}_{\{M_3 \geq T_4\}} \cdot M_4 \tag{34}$$

as derived from the model above and compute their expectation values. Again, MC simulations (with 100,000 sample points) and the PEM (with 163 sample points in case of $T_{\text{SpeedRestriction}}$ and 243 sample points in case of $T_{\text{LineClosure}}$) were applied. Figure 16 shows the results for several values of the inspection interval T_{inspect}.

As can be seen, the PEM reproduces correct trends compared to the MC results. But yet, the accuracy

Table 6. Repair time parameters for the extended degradation model based on the numbers in Table 7.

	R_1	R_2	R_3	R_4
μ_r	7.2218	2.9654	2.2830	−0.7128
σ_r	0.2119	0.2462	0.1980	0.1980

Table 7. Expert guess of mean repair time and standard deviations (SD) (in days).[22]

	R_1	R_2	R_3	R_4
Mean	1400	20	10	0.5
SD	300	5	2	0.1

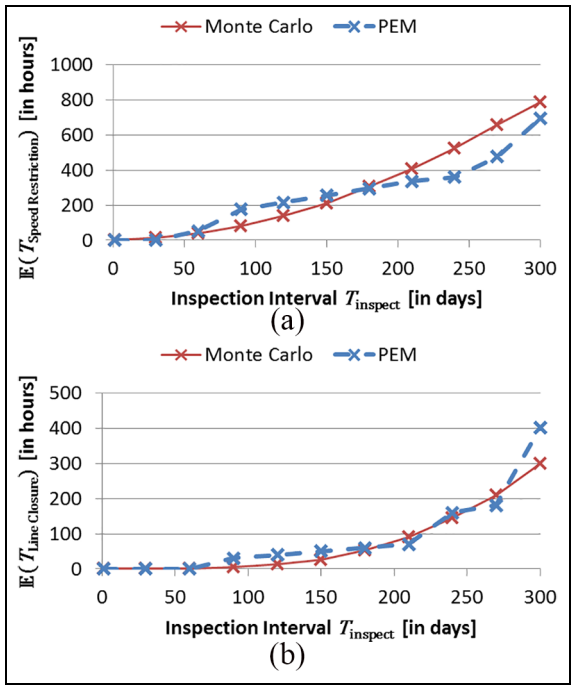

Figure 16. PEM results in comparison with standard MC simulations: (a) $\mathbb{E}(T_{\text{SpeedRestriction}})$ and (b) $\mathbb{E}(T_{\text{LineClosure}})$.

lacks behind that of the MC approach which mostly is because of the obvious discontinuity of the model functions from equations (33) and (34), as in the decision tree example from above. Nevertheless, remember the large difference concerning the number of sample points processed by the MC simulations in comparison with the PEM for generating the plots from Figure 16. Hence, if rough results are sufficient, the PEM still might be an appropriate approach in the context of models such as in Figure 15.

Conclusion

The examples from above show that the PEM is a very flexible approach that can successfully be applied to

various (but not all) types of models from railway asset management in order to analyze uncertainties in the model response in terms of the mean, variance, or even higher (centralized) moments. In contrast to common MC simulations, the described method usually (i.e. at least for small n) also requires the evaluation of only very few sample points. Thus, the computational load when assessing uncertainties in the model response can be considerably reduced in many cases, namely, if running the model under consideration for given realizations of its input vector is computationally expensive because of potentially complex calculations needed or simply because of large modeling scales.

Moreover, the PEM provides exact results whenever it is applied to polynomial functions (with a given maximum degree), whereas the MC approach necessarily yields approximate numbers only. On the contrary, MC simulations always converge toward the exact solution whenever the sample used is sufficiently large—whatever "sufficiently large" means depending on the specific situation—while there is no such guarantee or indicator for the accuracy of the PEM, in general. Thus, PEM results always have to be analyzed carefully—perhaps even more carefully than standard MC results—in order to avoid misinterpretations of the findings as well as wrong or at least inefficient decisions in practical applications. Consequently, a reasonable procedure in practice could be validating the accuracy of the PEM for the specific model under consideration once in a first step using more or less extensive MC simulations as a reference. Next, if successful, apply it to similar models on a larger scale usually without the need of further computationally expensive MC simulations.

Note that another critical aspect of the PEM (as described above) is that it requires stochastically independent input variables $X_1, \ldots X_n$. That means if some X_i for $i = 1, \ldots, n$ are correlated, one has to try out other tools[29] or make suitable adjustments to the present approach by, for example, using alternative transformation functions[30,31] (cf. Table 1) before applying the general PEM scheme from equation (8). Moreover, further approaches in combination with the PEM (e.g. polynomial chaos expansion[16,32]) are able to produce approximations for the complete cumulative distribution functions of the model response instead of basic statistics (i.e. mean, variance, etc.) only. Thus, overall, the PEM becomes an interesting and efficient alternative to standard MC simulations in various situations when it is applied carefully with awareness of the natural limitations of the approach.

Acknowledgements

The authors acknowledge the partners involved in the activities "Integrated modelling—Dynamic track geometry modelling" within In^{2}Rail project (HORIZION 2020, European research program) for their active and technical support and collaboration: Claudia Fecarotti and John Andrews (University of Nottingham, UK), Henk Samson (Strukton Rail, NL), and Benoit Guyot (SNCF Réseau, FR). Furthermore, the authors would like to thank the anonymous reviewers for their valuable comments that helped to significantly improve the quality of the original manuscript.

Declaration of conflicting interests

The author(s) declared no potential conflicts of interest with respect to the research, authorship, and/or publication of this article.

Funding

The author(s) disclosed receipt of the following financial support for the research, authorship, and/or publication of this article: This work was partially supported by the European Commission through its HORIZON 2020 research and innovation program during the In^{2}Rail project (Grant Agreement No. 635900).

ORCID iD

Thorsten Neumann https://orcid.org/0000-0002-9236-0585

References

1. Atamuradov V, Medjaher K, Dersin P, et al. Prognostics and health management for maintenance practitioners—review, implementation and tools evaluation. *Int J Progn Health Manage* 2017; 8: 31.
2. IEEE 1856-2017. IEEE standard framework for prognostics and health management of electronic systems.
3. Rezvanizaniani SM, Liu Z, Chen Y, et al. Review and recent advances in battery health monitoring and prognostics technologies for electric vehicle (EV) safety and mobility. *J Power Sources* 2014; 256: 110–124.
4. Kandukuri ST, Klausen A, Karimi HR, et al. A review of diagnostics and prognostics of low-speed machinery towards wind turbine farm-level health management. *Renew Sust Energ Rev* 2016; 53: 697–708.
5. Coble J, Ramuhalli P, Bond L, et al. A review of prognostics and health management applications in nuclear power plants. *Int J Progn Health Manage* 2015; 6: 33.
6. Ko JM and Ni YQ. Technology developments in structural health monitoring of large-scale bridges. *Eng Struc* 2005; 27: 1715–1725.
7. Meier-Hirmer C, Riboulet G, Sourget F, et al. Maintenance optimization for a system with a gamma deterioration process and intervention delay: application to track maintenance. *Proc ImechE, Part O: J Risk and Reliability* 2009; 223: 189–198.
8. Soleimanmeigouni I, Ahmadi A and Kumar U. Track geometry degradation and maintenance modelling: a review. *Proc ImechE, Part F: J Rail and Rapid Transit* 2018; 232: 73–102.
9. Higgins C and Liu X. Modeling of track geometry degradation and decisions on safety and maintenance: a literature review and possible future research directions. *Proc*

ImechE, Part F: J Rail and Rapid Transit 2018; 232: 1385–1397.
10. Fecarotti C. Optimisation of maintenance strategies for railway networks. In: *1st European railway asset management symposium*, Nottingham, UK, 27–28 March 2018. Nottingham, UK: University of Nottingham.
11. Bemment SD, Goodall RM, Dixon R, et al. Improving the reliability and availability of railway track switching by analysing historical failure data and introducing functionally redundant subsystems. *Proc ImechE, Part F: J Rail and Rapid Transit* 2018; 232: 1407–1424.
12. Silmon JA and Roberts C. Improving railway switch system reliability with innovative condition monitoring algorithms. *Proc ImechE, Part F: J Rail and Rapid Transit* 2010; 224: 293–302.
13. Bukhsh ZA, Saeed A and Stipanovic I. A machine learning approach for maintenance prediction of railway assets. In: *Transport research arena 2018*, Vienna, 16–19 April 2018.
14. Ghofrani F, He Q, Goverde RMP, et al. Recent applications of big data analytics in railway transportation systems: a survey. *Transp Res Part C: Emerg Technol* 2018; 90: 226–246.
15. Binder K and Heermann D. *Monte Carlo simulation in statistical physics: an introduction*. 5th ed. Berlin: Springer, 2010.
16. Schenkendorf R. A general framework for uncertainty propagation based on point estimate methods. In: *2nd European conference of the prognostics and health management society*, Nantes, 8–10 July 2014. PHM Society.
17. Schenkendorf R. *Optimal experimental design for parameter identification and model selection*. PhD Thesis, Otto-von-Guericke University Magdeburg, Magdeburg, 2014.
18. Isukapalli SS. *Uncertainty analysis of transport-transformation models*. PhD Thesis, Rutgers University, New Brunswick, NJ, 1999.
19. Andrews J. A modelling approach to railway track asset management. *Proc ImechE, Part F: J Rail and Papid Transit* 2012; 227: 56–73.
20. Andrews J, Prescott D and De Rozières F. A stochastic model for railway track asset management. *Reliab Eng Syst Safe* 2014; 130: 76–84.
21. Le B, Andrews J and Fecarotti C. A Petri net model for railway bridge maintenance. *Proc ImechE, Part O: J Risk and Reliability* 2017; 231: 306–323.
22. In2Rail Project. Deliverable D6.*8 report on technical validation of concepts and models*, http://www.in2rail.eu/Page.aspx?CAT=DELIVERABLES&IdPage=69d2e365-3355-45d4-bb3c-5d4ba797a3ac (accessed 24 September 2018).
23. Zacks S. *Introduction to reliability analysis*. New York: Springer, 1992.
24. Bell MGH and Iida Y. *Transportation network analysis*. Chichester: Wiley, 1997.
25. Schenkendorf R and Böhm T. Aspekte einer datengetriebenen, zustandsabhängigen Instandhaltung: (Teil 3) Zustandsdiagnose und -prognose. *EI—Der Eisenbahningenieur* 2015; 5: 43–49.
26. Yang C and Létourneau S. Two-stage classifications for improving time-to-failure estimates: a case study in prognostic of train wheels. *Appl Intell* 2009; 31: 255–266.
27. Song YY and Lu Y. Decision tree methods: applications for classification and prediction. *Shanghai Arch Psychiatry* 2015; 27: 130–135.
28. Audley M and Andrews JD. The effects of tamping on railway track geometry degradation. *Proc ImechE, Part F: J Rail and Rapid Transit* 2013; 227: 376–391.
29. Zhu Y, Wang QA, Li W, et al. Analytic uncertainty and sensitivity analysis of models with input correlations. *Physica A* 2018; 494: 140–162.
30. Mandur J and Budman H. A polynomial-chaos based algorithm for robust optimization in the presence of Bayesian uncertainty. *IFAC P Vol* 2012; 45(15): 549–554.
31. Xie X, Krewer U and Schenkendorf R. Robust optimization of dynamical systems with correlated random variables using the point estimate method. *IFAC-PapersOnLine* 2018; 51(2): 427–432.
32. Le Maître O and Knio OM. *Spectral methods for uncertainty quantification: with applications to computational fluid dynamics*. Dordrecht: Springer, 2010.

Appendix I

Given f as in equation (28), the conditional equation

$$\mathbb{P}\big(f_i(X_1, X_2, X_3) = 1 | Z = z_j\big) = p_{ij} \tag{35}$$

(cf. equation (32)) for $i, j = 0, 1, 2$ can be solved easily as exemplarily shown for $i = j = 1$ in the following. For, in this case, the conditional distributions of X_1 and X_3 (given $Z = z_1$) are defined as $\mathcal{N}(0.6, 0.1)$ and $\mathcal{N}(0.35, 0.05)$, respectively, according to Table 5. Thus, by transformation, one obtains the random variables

$$\tilde{X}_1 := \frac{X_1 - 0.6}{0.1} \tag{36}$$

and

$$\tilde{X}_3 := \frac{X_3 - 0.35}{0.05} \tag{37}$$

both having a standard Gaussian distribution given $Z = z_1$. Moreover, note that X_1 and X_3 are conditionally independent given Z by assumption. Hence, equation (35) yields

$$\begin{aligned} p_{11} &= \mathbb{P}(f_1(X_1, X_2, X_3) = 1 | Z = z_1) \\ &= \mathbb{P}(X_1 > 0.496 \text{ and } X_3 \leqslant 0.532 | Z = z_1) \\ &= \mathbb{P}(X_1 > 0.496 | Z = z_1) \cdot \mathbb{P}(X_3 \leqslant 0.532 | Z = z_1) \\ &= \mathbb{P}\big(\tilde{X}_1 > -1.04 | Z = z_1\big) \cdot \mathbb{P}\big(\tilde{X}_3 \leqslant 3.64 | Z = z_1\big) \\ &= (1 - \Phi(-1.04)) \cdot \Phi(3.64) \\ &\approx 0.8508 \cdot 0.9998 \\ &= 0.8506 \end{aligned} \tag{38}$$

where Φ is the cumulative distribution function of the standard Gaussian distribution. The expected value and variance as in equations (30) and (31) are then directly given by $\mathbb{E}(f_1(X_1, X_2, X_3) | Z = z_1) = p_{11} \approx 0.8506$ and $\mathrm{Var}(f_1(X_1, X_2, X_3) | Z = z_1) = p_{11}(1 - p_{11}) \approx 0.1271$, respectively.